JOURNAL OF MAGNETIC RESONANCE IMAGING 37:853–859 (2013)

Original Research

Aortic Pulse Wave Velocity Measurements With Undersampled 4D Flow-Sensitive MRI: Comparison With 2D and Algorithm Determination

Andrew L. Wentland, MS,[1,2]* Oliver Wieben, PhD,[1,2] Chris J. François, MD,[2] Christina Boncyk, BS,[2] Alejandro Munoz Del Rio, PhD,[2] Kevin M. Johnson, PhD,[1] Thomas M. Grist, MD,[1,2] and Alex Frydrychowicz, MD[2,3]

Purpose: To compare pulse wave velocity (PWV) measurements obtained from radially undersampled 4D phase-contrast magnetic resonance imaging (PC-MRI) with 2D PC measurements and to evaluate four PWV algorithms.

Materials and Methods: PWV was computed from radially undersampled 3D, 3-directionally velocity-encoded PC-MRI (4D) acquisitions performed on a 3T MR scanner in 18 volunteers. High temporal resolution 2D PC scans serving as a reference standard were available in 14 volunteers. Four PWV algorithms were tested: time-to-upstroke (TTU), time-to-peak (TTP), time-to-foot (TTF), and cross-correlation (XCorr). Bland–Altman analysis was used to determine inter- and intraobserver reproducibility and to compare differences between algorithms. Differences in age and PWV measurements were analyzed with Student's *t*-tests. The variability of age-corrected data was assessed with a Brown-Forsythe analysis of variance (ANOVA) test.

Results: 2D (4.6–5.3 m/s) and 4D (3.8–4.8 m/s) PWV results were in agreement with previously reported values in healthy subjects. Of the four PWV algorithms, the TTU, TTF, and XCorr algorithms gave similar and reliable results. Average biases of +0.30 m/s and −0.01 m/s were determined for intra- and interobserver variability, respectively. The Brown-Forsythe test revealed that no differences in variability could be found between 2D and 4D PWV measurements.

Conclusion: 4D PC-MRI with radial undersampling provides reliable and reproducible measurements of PWV. TTU, TTF, and XCorr were the preferred PWV algorithms.

Key Words: 4D PC MRI; phase contrast; pulse wave velocity; radial undersampling
J. Magn. Reson. Imaging 2013;37:853–859.

NONINVASIVE TECHNIQUES and biomarkers for evaluating the progression of atherosclerosis are of great interest for diagnosis and treatment monitoring. Pulse wave velocity (PWV), the rate at which the systolic wave of blood traverses the vasculature, is one such biomarker, as it is indirectly indicative of vascular stiffness. As arteries become stiffer with age or due to the development from subclinical to clinically apparent atherosclerosis, PWV increases because of the loss of elastic recoil in the vessel (1). PWV increases independently with age and blood pressure (2) and is predictive of stroke irrespective of blood pressure (3).

PWV can be evaluated by detecting the temporal shift in blood flow waveforms at two or more locations in a vessel. Such measurements can be performed either invasively (pressure transducers) or noninvasively (applanation tonometry, ultrasound, magnetic resonance imaging [MRI]). Ultrasound-based carotid-to-femoral (artery) pulse wave velocity is a standard clinical procedure. However, distance measurements between these two locations are inaccurate and can lead to differences in PWV values of up to 30% (4).

Several MRI-based methods of measuring PWV have been reported in the literature. Most MR studies on PWV have been performed with the use of a 2D phase-contrast (PC) acquisition with (unidirectional) through-plane velocity encoding (5). In its most basic form, two locations separated by a known distance are used (6–9). Results rely on the temporal difference between the waveforms from the two locations and hence on the quality of waveform sampling (10,11). Examinations based on Fourier-

[1]Department of Medical Physics, University of Wisconsin School of Medicine and Public Health, Madison, Wisconsin, USA.
[2]Department of Radiology, University of Wisconsin School of Medicine and Public Health, Madison, Wisconsin, USA.
[3]Clinic for Radiology and Nuclear Medicine, University Hospital Schleswig-Holstein, Lübeck, Germany.

Contract grant sponsor: UW Department of Radiology R&D Funds; Contract grant sponsor: NHLBI Ruth L. Kirschstein National Research Service Award for Individual Predoctoral MD/PhD Fellows; Contract grant number: F30 HL108539-02; Contract grant sponsor: National Institutes of Health (NIH) Medical Scientist Training Program.

*Address reprint requests to: A.L.W., University of Wisconsin School of Medicine & Public Health, Department of Medical Physics, 1111 Highland Ave., Madison, WI, 53705-2275. E-mail: alwentland@wisc.edu

Received May 10, 2012; Accepted September 12, 2012.
DOI 10.1002/jmri.23877
View this article online at wileyonlinelibrary.com.

velocity-encoded MRI produce time-velocity profiles with very high temporal resolution, on the order of 3.5 msec (12,13). However, curvatures within the vasculature limit this approach, which is of particular concern since vessels tend to become tortuous with disease (14).

Recently, time-resolved 3D (so-called "4D") PC MRI approaches with volumetric coverage and velocity sensitivity in all three spatial directions have been presented (15,16). A volumetric approach to PC MRI could help to overcome patient-specific and/or methodological limitations in 2D PWV measurements, such as potentially tedious slice placement in 2D approaches, especially in tortuous vessels. However, the achievable temporal resolution is inherently lower in 4D PC MRI because of the three-directional velocity encoding employed. A previously described Cartesian 4D PC MRI approach to PWV measurements provided thick-slab volumetric coverage with three-directional flow encoding. This technique has shown great potential, but at the expense of long scan times (15–20 minutes), compromised temporal resolution (>40 msec), and no validation against a clinical standard or other MRI-based measurement of PWV (11).

Several algorithms for computing PWV have been proposed in the literature (6,9,11,17–19), such as the time-to-peak (TTP), time-to-foot (TTF), cross-correlation (XCorr), and second-derivative time-to-upstroke (TTU) algorithms. For studies comparing different algorithms, either the TTF (11) or the XCorr (17) algorithms were the most reliable.

PC MRI with vastly undersampled isotropic projection reconstruction (PC VIPR) applies radial undersampling (20) to address a few of the technical limitations of the Cartesian approach. It offers increased spatial and temporal resolution with large volume coverage in reduced scan times at the cost of acceptable artifacts (15,21). The purpose of this prospective study was to compare PWV based on 4D velocity data acquired with PC VIPR to a high temporal resolution 2D approach as the reference standard. We hypothesized that the 4D technique would provide PWV measurements of equivalent magnitude and variability to the 2D approach. For both techniques, PWV calculations were based on previously reported algorithms, including the TTP, TTF, XCorr, and TTU algorithms. Secondary aims included the analysis of PWV differences between age groups (volunteers < and >35 years of age) and the determination of the most suitable algorithm(s) for calculating PWV.

MATERIALS AND METHODS

Subjects

Twenty healthy volunteers were included in this Health Insurance Portability and Accountability Act (HIPAA)-compliant study. The study protocol was approved by the local Institutional Human Subjects Review Board (IRB). Written informed consent was obtained from all subjects prior to inclusion. As part of the inclusion criteria, volunteers had to meet the following criteria: 1) No history of cardiovascular disease, 2) no history of smoking, 3) no cardiovascular medication, and 4) a body mass index (BMI) $\leq$30 kg/m^2. Data for two subjects were retrospectively excluded from the study for gating failures: one subject presented with a previously undiagnosed arrhythmia that led to erroneous electrocardiogram (ECG) triggering. Similarly, the data for the second subject was invalid due to faulty ECG and respiratory triggering. Furthermore, in four of the 18 2D PC MRI datasets, the cardiac trigger was sufficiently delayed such that the systolic upstroke of the flow waveform was never sampled. These four 2D datasets were excluded from the study. All comparisons between 2D and 4D data used the remaining 14 subjects (seven men, seven women, ages 22–59 years, mean age [±1 SD]: 34.0 ± 13.5 years). In analyses performed on 4D data alone, data were used from all 18 healthy volunteers (nine men, nine women, ages 22–60 years, mean age [±1 SD]: 38.4 ± 14.8 years; mean BMI: 25.6 ± 3.5 kg/m^2).

MRI

4D PC VIPR data were acquired on a 3T clinical MR scanner (MR750, GE Healthcare, Waukesha, WI) using a 32-channel torso coil (NeoCoil, Pewaukee, WI). A dual-echo 5-point velocity encoded sequence with retrospective ECG-gating was used (22). Typical scan parameters were: V_{enc} = 150 cm/s, TR/TE = 6.4–6.7/2.2 msec, flip angle = 20–22°, bandwidth = 488.3 Hz/pixel, readout = 256 samples, resulting in 1.25 mm^3 isotropic spatial resolution. The acquisition was conducted with an axial excitation that provided an imaging volume of 32 × 32 × 22 cm^3 with selective excitation in the superior-to-inferior direction. Respiratory gating with a 50% acceptance window that continuously adapts to the expiration position was used. The PC VIPR scan time was on the order of 11.5 minutes. During postprocessing, time frames were reconstructed with temporal filtering in the RR-cycle, similar to view sharing in Cartesian acquisitions; this reconstruction provided time frames of 32–33.5 msec duration (23,24). This temporal filter provides a temporal window equal to 5*TR (32–33.5 msec) in the lower frequency regions of *k*-space and widens for higher spatial frequencies to a maximum of 25*TR (160–167.5 msec) in the outer regions of *k*-space. Depending on each individual's heart rate (range: 49–72 bpm; mean [±1 SD]: 55.5 ± 6.5 bpm), data were reconstructed to 30.3 ± 3.6 time frames/cardiac cycle.

A commercial 2D PC sequence with prospective ECG-gating was applied in four scan planes placed orthogonal to the main flow direction in the ascending aorta, aortic arch, and in the proximal and supra-diaphragmatic descending aorta. Scan parameters included: V_{enc} = 150 cm/s, TR/TE = 5.2/3.0 msec, flip angle = 30°, matrix size 256 × 256 pixels, slice thickness = 7 mm, in-plane spatial resolution = 1.6 × 1.6 mm^2, 54.3 ± 21.2 time frames, temporal resolution = ~10.4 msec. The choice of four slices provides data from each section of the thoracic aorta and provides a low number of planes to minimize the scan

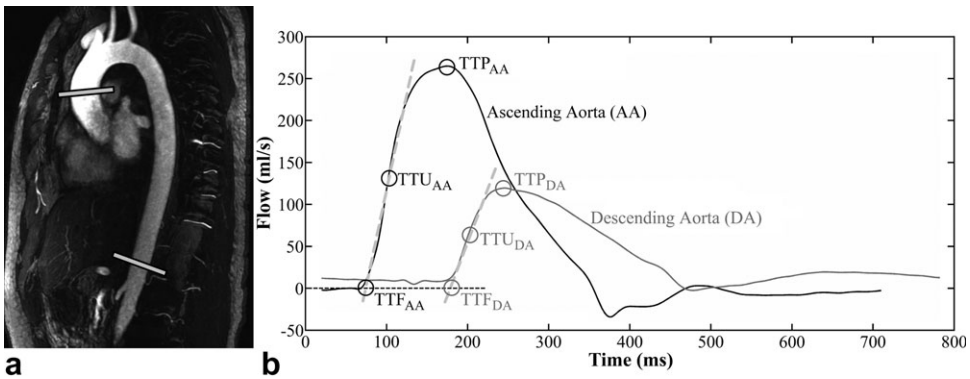

Figure 1. A contrast-enhanced angiogram (**a**) with representative planes in the ascending and descending aorta. Flow waveforms (**b**) from the two planes are shown with the TTU, TTF, and TTP algorithms. The best fit linear lines along the upstroke were used to identify the foot of the waveforms. Please note that the two planes shown in (**a**) are used to represent the two waveforms shown in (**b**). In this study, four planes were used in the 2D approach and six planes were used in the 4D approach.

time required for the 2D evaluation of PWV. A contrast-enhanced MR angiogram with 0.03 mmol/kg gadofosveset trisodium (Ablavar, Lantheus, Billerica, MA) injected at 0.6 mL/s followed by a 30-mL saline chaser was performed per clinical standard to guide placement of the 2D planes (25).

Data Analysis

A MATLAB-based software tool (MathWorks, Natick, MA) was developed to perform the PWV calculations from 2D and 4D data. For 2D data, regions of interest (ROIs) were interactively drawn within the vessel lumen to measure the flow waveform. The distance calculation between the four scan planes was based on a double-oblique reformatted slice of the CE-MRA data ("candy cane" view, Fig. 1). To compute a vessel centerline, the user placed a series of points in the approximate center of the vessel along the length of the aorta. A spline interpolation was created from this set of points to approximate a vessel centerline. The intersection of the centerline with each individual 2D PC plane was used for distance calculations.

To analyze the 4D data, six planes slightly larger than the diameter of the aorta were manually placed double-obliquely such that a cross-sectional axial view of the aorta could be extracted from the 4D dataset. These planes were placed in evenly spaced distances using a time-averaged surface shaded display of the aorta created from the PC angiogram. The exact distances between planes were determined by computing the centroid of each plane and calculating distances between centroids along a 3D cubic spline interpolant that functioned as a vessel centerline. Six planes along the thoracic aorta was an adequate number of planes to compute the spline centerline. A fewer number of planes led to a spline that significantly deviated from the vessel center. Additionally, the six planes used in the 4D analysis covered the same superior-to-inferior distance along the aorta that was covered by the four planes used with the 2D approach above.

Flow waveforms were upsampled to 400 points via spline interpolation. Temporal shifts in the flow waveforms between planes were determined with four algorithms (Fig. 1): TTU, TTP, TTF, and XCorr. The TTP, TTF, and XCorr algorithms were computed as previously described (11). Similar to previously proposed derivative methods of computing PWV (18), TTU was defined as the point of maximum acceleration on the upstroke of the waveform. As described previously (11), the distances between planes were plotted versus the time shifts computed from the TTU, TTP, TTF, and XCorr algorithms. A linear line was fitted to the data and the PWV was computed as the inverse slope of this line.

Statistical Analysis

Since neither test represents an established gold standard, 2D and 4D PWV calculations were compared following Bland and Altman analysis (26) for each of the four algorithms (TTU, TTP, TTF, and XCorr). The bias ± 2 SD was reported for each comparison and as an average for both the 2D and 4D approaches. 2D and 4D measurements were also compared with a paired Student's *t*-test. Inter- and intraobserver reproducibility of the 4D data was evaluated for 10/18 randomly chosen subjects and assessed with Bland–Altman analysis. The reproducibility of PWV measurements depends on several factors, including the slice selection and the placement of ROIs. Given that the slice selection of 2D data was performed at the time of acquisition, the reproducibility of 2D data was not assessed because the a priori selection of 2D slices mitigates true differences in repeated measurements from 2D data.

Since four algorithms were evaluated in this study, it was of interest to assess and compare the variability of each algorithm. Given the relationship between PWV and age irrespective of blood pressure and other atherosclerotic risk factors (2), regression models of PWV on age and its square (age^2) were fitted to the data; the coefficient of determination R^2 was used to

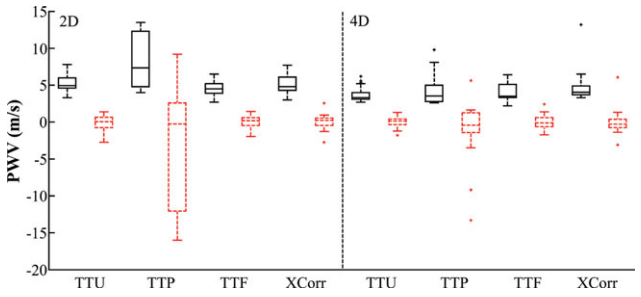

Figure 2. Boxplots of PWV measurements as calculated from 2D PC slices and 4D PC VIPR datasets. The vertical axis was scaled around the boxplots; two outliers (at 30.5 and 74.5 m/s) for the 2D TTP measurements lie outside of this range and are not shown in this graph. Raw data are plotted with solid lines; age-adjusted values are plotted with dashed red lines.

assess the percentage of variance in the response explained by the model. The results were plotted next to the raw data results; the shift between raw data and adjusted data represents the influence of age. This age adjustment thus allows for a comparison of the variability of the 2D and 4D PWV measurements despite the large age range (22–60 years) of our subjects. Differences in variability between 2D and 4D were assessed by a Brown-Forsythe analysis of variance (ANOVA) test.

To reveal physiological changes with age, data were separated into two groups based on age: subjects $\leq$35 years of age and subjects >35 years of age. Data between age groups were tested for differences with an unpaired Student's *t*-test ($P < 0.05$) for each method of analysis for both the 2D and 4D datasets.

The criterion for statistical significance was $P < 0.05$ (two-sided). There was no adjustment of *P*-values for multiple testing. Statistical analyses were performed in R 2.12.1 (R Development Core Team 2010).

RESULTS

Figure 2 shows the mean and standard deviation of the PWV measurements as calculated from 2D PC slices and 4D PC VIPR datasets. 2D and 4D PWV data were similar in magnitude and spread, except for values calculated with the TTP algorithm (Fig. 2; solid boxplots). Given the high degree of variability of the TTP data and nonphysiological results, the TTP algorithm was deemed to be unreliable and results were excluded from the subsequent, more detailed analyses.

Overall, mean 4D PWV ($n = 18$) measurements ranged from 3.8–4.8 m/s, whereas mean 2D PWV ($n = 14$) measurements were greater and ranged from 4.6–5.3 m/s (Table 1). In a direct comparison of 2D and 4D results in 14 subjects, the mean PWV ranged from 3.5–4.2 m/s for the 4D data and from 4.6–5.3 m/s for the 2D data (Table 1). Bland–Altman analysis in these 14 subjects confirmed that 2D PWV measurements tended to be greater than 4D PWV measurements, with bias and 95% limits of agreement (average bias ±2 SD) of +1.8 ± 3.15, +0.68 ± 3.98, and +0.84 ± 3.37 m/s for the TTU, TTF, and XCorr algorithms, respectively (Fig. 3). However, only TTU calculations showed significantly greater values for 2D than for 4D PWV measurements ($P < 0.001$; Table 1). For the 4D data ($n = 10$), interobserver reproducibility provided an overall mean (±2 SD) bias of +0.30 ± 2.83 m/s and intraobserver reproducibility provided an overall mean (±2 SD) bias of −0.01 ± 2.51 m/s (Fig. 4; Table 1).

Boxplots of the residuals of an age and age^2 regression model to the data demonstrated that some of the variability of the data (R^2 ranging from 11% to 46%) could be accounted for by the age of the subject (Fig. 2; dashed red boxplots). To test for differences in the variability of all eight groups in Fig. 2, the Brown-Forsythe test demonstrated a *P*-value of 1.1×10^{-6}, indicating that one of the sets of measurements was significantly more variable than others. The residuals of the TTP data were visibly more variable than measurements computed from the other methods (Fig. 2); removal of the TTP data from the Brown-Forsythe test demonstrated a *P*-value of 0.609, implying no significant differences in variability could be found between 2D and 4D measurements with the TTU, TTF, and XCorr algorithms, which justified the initial exclusion of TTP data.

For 4D PWV data grouped by ages of $\leq$35 and >35 years of age, the TTU ($P = 0.02$) and XCorr ($P = 0.048$) algorithms demonstrated expected increases with age, whereas no trend with age could be found for the TTF ($P = 0.42$) data. No age/PWV relationships could be found in the 2D PWV data ($P \geq 0.073$).

DISCUSSION

The results of this study demonstrate the feasibility of measuring global aortic PWV with the radially

Table 1
PWV Results From 2D and 4D Data Based on Four Different Algorithms

Algorithm	4D ($n = 18$)	2D ($n = 14$)	4D ($n = 14$)	Bias ± 2 SD ($n = 14$)	2D vs. 4D *P*-values	4D intraobserver bias ± 2 SD ($n = 10$)	4D Interobserver bias ± 2 SD ($n = 10$)
TTU	3.8 ± 1.1	5.3 ± 1.3	3.5 ± 0.9	+1.8 ± 3.15	**0.001**	+0.15 ± 2.82	+0.40 ± 2.67
TTP	5.0 ± 10.8	14.1 ± 18.7	4.2 ± 2.0	+9.86 ± 35.9	0.054	−3.77 ± 18.6	−4.37 ± 21.8
TTF	4.0 ± 1.1	4.6 ± 1.1	3.9 ± 1.2	+0.68 ± 3.98	0.224	−0.10 ± 3.26	+0.78 ± 3.29
XCorr	4.8 ± 2.3	5.1 ± 1.4	4.2 ± 0.9	+0.84 ± 3.37	0.086	−0.09 ± 1.22	−0.27 ± 2.31

Except for *P*-values, values shown are in m/s. Significant *P*-values are shown in bold. TTU = time-to-upstroke; TTP = time-to-peak; TTF = time-to-foot; XCorr = cross-correlation; SD = standard deviation.

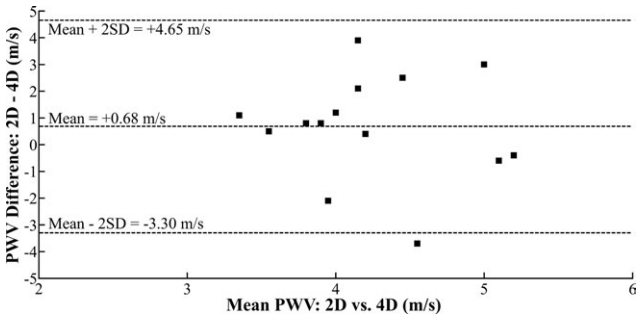

Figure 3. Bland–Altman analysis of the 2D vs. 4D PWV results computed with the TTF algorithm. PWV measurements from 2D PC data tended to be higher, with an average bias (±2 SD) of +0.68 ± 3.98 m/s.

undersampled 4D flow-sensitive MRI technique, PC VIPR. While numerous studies have used MRI to evaluate PWV, this is the first study to perform such measurements with a radially undersampled 4D technique in a reasonable scan time without a sacrifice in spatial resolution or field of view. The 4D-based PWV measurements performed in this study were of similar magnitude to values reported in the literature (11,17) and were of equal variability and similar magnitude to our reference 2D PWV measurements. Without a practical noninvasive "gold standard" to compare these MRI-based PWV measurements, no conclusions can be made regarding the superiority or inferiority of the 4D technique for measuring PWV. Since 2D-based PWV measurements have been established as a reliable technique (9), the purpose of this study was to assess whether a 4D radially undersampled technique could estimate PWV reliably. Such an investigation is necessary given the 4D acquisition's lower temporal resolution compared to 2D approaches and the reduced scan time relative to other flow-sensitive 4D techniques (11). While the 4D PC VIPR acquisition still requires 11.5 minutes of scan time, the acquisition of multiple 2D slices along with an angiogram is time-consuming due to the prescription of double-oblique planes and the recovery periods needed between successive breath-holds. Furthermore, the analysis time for 2D and 4D PWV measurements was similar as well.

The PC VIPR technique provides several advantages aside from the ability to analyze the data with regard to PWV: PC VIPR does not rely on accurate slice prescriptions and also provides perfectly coregistered anatomical, angiographic, and three-directional flow information over a large volume, which can be qualitatively and quantitatively evaluated. Knowledge of the three-directional velocity information can be used to calculate other hemodynamic parameters, such as wall shear stress, oscillatory shear index, pressure gradients, turbulence, kinetic energy, and others. Therefore, the ability to characterize PWV with PC VIPR would be an additional useful parameter that could be derived from a single PC VIPR acquisition. M-mode-based MR imaging has superior temporal resolution (~3.5 msec), shorter scan times (~2 min) (12), and allows for regional PWV measurements, but only in a straight segment of the aorta. PWV measurements derived from the 4D technique in this study can be used for the whole aortic arch and can account for variations in vascular anatomy; however, the regional assessment of PWV is a significant challenge due to the limited temporal resolution of 4D PC MRI approaches.

TTP PWV measurements were the most variable and most prone to extremely aberrant, nonphysiological values. TTP PWV is largely dependent on the systolic peak of the waveform, and hence, highly reliant on sufficient temporal resolution to detect the true systolic peak. In addition, reflected pressure waves and noise contributions may have contributed to errors in the peak time from one plane to the next, making it the least robust algorithm of the methods tested here; this is in accordance with previous studies assessing TTP versus other algorithms (11,17). Similarly for the 4D TTP calculations, the markedly lower temporal resolution of the PC VIPR technique may have increased uncertainty in sampling the true peak of the waveform in one plane but not another, leading to unreliable 4D TTP measurements.

TTU and TTF measurements rely on multiple points in the flow waveform and are thus less sensitive to temporal undersampling and noise. Additionally, the timepoints needed for TTU and TTF measurements are likely earlier in the flow waveform compared to timepoints affected by reflected waves. As XCorr measurements inherently use the entire waveform, XCorr is likely less susceptible to the effects of trigger delays and noise. As a result of these insensitivities, the TTU, TTF, and XCorr algorithms provided similar

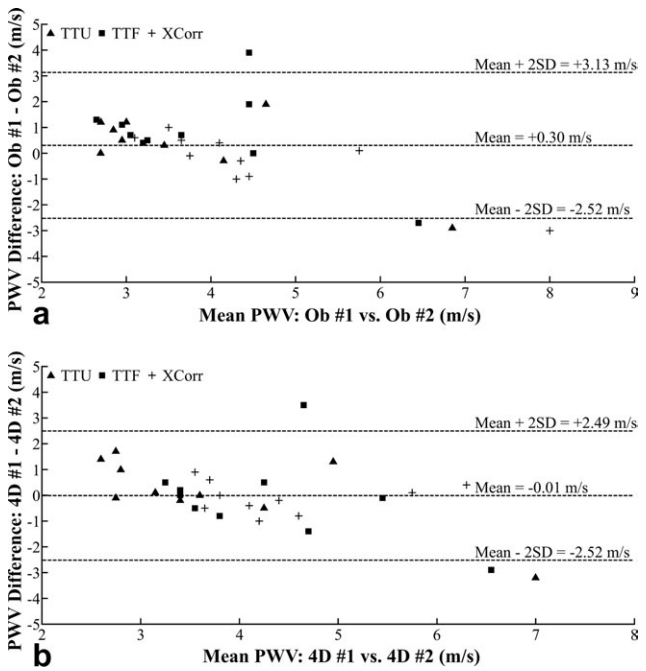

Figure 4. Bland–Altman plots for inter- (**a**) and intraobserver (**b**) reproducibility of 4D PWV measurements. Interobserver reproducibility provided a mean (±2 SD) bias of +0.30 ± 2.83 m/s and intraobserver reproducibility provided a mean (±2 SD) bias of −0.01 ± 2.51 m/s.

magnitude and variability. Given that occasional outliers occur with all of the PWV algorithms, we advocate a multi-algorithm approach to PWV measurements that includes the TTU, TTF, and XCorr algorithms. Thus, an extreme value from one algorithm can be compensated for by the similarity between values from the remaining algorithms. A multi-algorithm approach to PWV measurements requires at least three algorithms; if only two algorithms are used and the values from each are substantially different, it is unknown which number can be trusted, if any. Given the unreliability of the TTP algorithm, an algorithm was needed in addition to the TTF and XCorr algorithms that have been established in the literature. The TTU algorithm provides the third measurement in the multi-algorithm approach.

The ~32 msec temporal resolution of the PC VIPR sequence is a limitation of the study and could be insufficient to resolve differences for diseased subjects with PWV values greater than 5 m/s. The lower temporal resolution of the PC VIPR technique may also explain why average PWV values were lower than with the 2D approach to PWV measurements. Since this study did not include diseased subjects, we are uncertain of the ability of our 4D PWV technique to detect values greater than 5 m/s, given that this was the greatest value detected in this study. In future studies with diseased subjects and elevated pulse wave velocities, analysis planes may need to be placed further apart from one another to resolve the differences in waveform characteristics. Although our 4D PWV measurements were not compared to the gold standard invasive pressure measurements, our method was compared to 2D PWV measurements, which have been validated previously with invasive pressure measurements (9). While four planes were used to measure PWV with 2D data, six analysis planes were used to compute PWV with the 4D data due to the centerline algorithm employed in our analysis tool. Although the number of analysis planes is different between the 2D and 4D approaches, the spatial extent of the planes was the same for measuring global aortic PWV. Nevertheless, this limitation could be avoided with the use of an alternative algorithm for computing the vessel centerline. Despite having strict inclusion criteria in terms of BMI and history of smoking and cardiovascular disease, our subjects spanned a large age range. While our analysis of variability accounted for variation due to age, a study with subjects in a narrower age range would be useful for more thoroughly comparing the variability of the TTU, TTF, and XCorr algorithms. Although a degree of bias was found in comparing the 2D and 4D PWV measurements (on the order of 0.68–1.8 m/s), the differences were relatively small. Such small differences are unlikely to affect clinical decisions based on PWV measurements because diseased subjects are likely to have a PWV that is approximately double the PWV of a normal subject (2).

Problems with cardiac gating led to a reduction in the number of cases included in the 2D to 4D comparison. As with all functional cardiovascular MR, sequences rely on proper gating. The two subjects with poor cardiac gating thus led to the improper acquisition of data. An additional problem with cardiac gating was met with the 2D acquisition. With the use of prospective cardiac gating, flow waveforms measured from slices acquired proximal to the heart were occasionally missing part of early systole. Since prospective gating requires a trigger from the QRS complex, the electrical delay between this trigger time and the acquisition led to the absence of the upstroke in slices through the ascending aorta and aortic arch. Such delays could be the result of a higher heart rate, a truly elevated pulse wave velocity, or anatomical differences that shorten the distance the systolic bolus needs to travel to the plane of interest. Without the upstroke, algorithms like TTF and TTU cannot function properly. Since the PC VIPR acquisition was retrospectively cardiac gated, no data were missing from the flow waveforms. In future studies, retrospectively gated 2D PC acquisitions or Fourier-encoded data in straight vessel segments should be used as reference standards.

In conclusion, the 4D PC VIPR acquisition is a promising means of obtaining PWV measurements. The 4D PWV results included in this study were similar in magnitude and variability to values in the literature and to our reference 2D PWV results for the TTU, TTF, and XCorr algorithms. Low inter- and intraobserver variability for the 4D approach lends credence to its use in future clinical applications. Further studies with the 4D technique are warranted, including studies in patients with variable disease severity, elevated PWV, and across a more complete spectrum of ages.

REFERENCES

1. Bock M, Schad LR, Muller E, Lorenz WJ. Pulsewave velocity measurement using a new real-time MR-method. Magn Reson Imaging 1995;13:21–29.
2. [No authors listed.] Determinants of pulse wave velocity in healthy people and in the presence of cardiovascular risk factors: 'establishing normal and reference values.' Eur Heart J 2010;31: 2338–2350.
3. Laurent S, Katsahian S, Fassot C, et al. Aortic stiffness is an independent predictor of fatal stroke in essential hypertension. Stroke 2003;34:1203–1206.
4. Salvi P, Magnani E, Valbusa F, et al. Comparative study of methodologies for pulse wave velocity estimation. J Hum Hypertens 2008;22:669–677.
5. Mohiaddin RH, Firmin DN, Longmore DB. Age-related changes of human aortic flow wave velocity measured noninvasively by magnetic resonance imaging. J Appl Physiol 1993;74:492–497.
6. Boese JM, Bock M, Schoenberg SO, Schad LR. Estimation of aortic compliance using magnetic resonance pulse wave velocity measurement. Phys Med Biol 2000;45:1703–1713.
7. Stevanov M, Baruthio J, Gounot D, Grucker D. In vitro validation of MR measurements of arterial pulse-wave velocity in the presence of reflected waves. J Magn Reson Imaging 2001;14: 120–127.
8. Laffon E, Marthan R, Montaudon M, Latrabe V, Laurent F, Ducassou D. Feasibility of aortic pulse pressure and pressure wave velocity MRI measurement in young adults. J Magn Reson Imaging 2005;21:53–58.
9. Grotenhuis HB, Westenberg JJ, Steendijk P, et al. Validation and reproducibility of aortic pulse wave velocity as assessed with velocity-encoded MRI. J Magn Reson Imaging 2009;30:521–526.
10. Bolster BD, Jr., Atalar E, Hardy CJ, McVeigh ER. Accuracy of arterial pulse-wave velocity measurement using MR. J Magn Reson Imaging 1998;8:878–888.

11. Markl M, Wallis W, Brendecke S, Simon J, Frydrychowicz A, Harloff A. Estimation of global aortic pulse wave velocity by flow-sensitive 4D MRI. Magn Reson Med 2010;63:1575–1582.
12. Taviani V, Hickson SS, Hardy CJ, et al. Age-related changes of regional pulse wave velocity in the descending aorta using Fourier velocity encoded M-mode. Magn Reson Med 2011;65:261–268.
13. Hardy CJ, Bolster BD Jr, McVeigh ER, Iben IE, Zerhouni EA. Pencil excitation with interleaved fourier velocity encoding: NMR measurement of aortic distensibility. Magn Reson Med 1996;35: 814–819.
14. Mochida M, Sakamoto H, Sawada Y, et al. Visceral fat obesity contributes to the tortuosity of the thoracic aorta on chest radiograph in poststroke Japanese patients. Angiology 2006;57:85–91.
15. Gu T, Korosec FR, Block WF, et al. PC VIPR: a high-speed 3D phase-contrast method for flow quantification and high-resolution angiography. AJNR Am J Neuroradiol 2005;26:743–749.
16. Markl M, Chan FP, Alley MT, et al. Time-resolved three-dimensional phase-contrast MRI. J Magn Reson Imaging 2003;17: 499–506.
17. Fielden SW, Fornwalt BK, Jerosch-Herold M, Eisner RL, Stillman AE, Oshinski JN. A new method for the determination of aortic pulse wave velocity using cross-correlation on 2D PCMR velocity data. J Magn Reson Imaging 2008;27:1382–1387.
18. Taviani V, Patterson AJ, Graves MJ, et al. Accuracy and repeatability of fourier velocity encoded M-mode and two-dimensional cine phase contrast for pulse wave velocity measurement in the descending aorta. J Magn Reson Imaging 2010;31:1185–1194.
19. Rogers WJ, Hu YL, Coast D, et al. Age-associated changes in regional aortic pulse wave velocity. J Am Coll Cardiol 2001;38: 1123–1129.
20. Peters DC, Korosec FR, Grist TM, et al. Undersampled projection reconstruction applied to MR angiography. Magn Reson Med 2000;43:91–101.
21. Johnson KM, Lum DP, Turski PA, Block WF, Mistretta CA, Wieben O. Improved 3D phase contrast MRI with off-resonance corrected dual echo VIPR. Magn Reson Med 2008;60:1329–1336.
22. Johnson KM, Markl M. Improved SNR in phase contrast velocimetry with five-point balanced flow encoding. Magn Reson Med 2010;63:349–355.
23. Du J, Carroll TJ, Brodsky E, et al. Contrast-enhanced peripheral magnetic resonance angiography using time-resolved vastly undersampled isotropic projection reconstruction. J Magn Reson Imaging 2004;20:894–900.
24. Liu J, Redmond MJ, Brodsky EK, et al. Generation and visualization of four-dimensional MR angiography data using an undersampled 3-D projection trajectory. IEEE Trans Med Imaging 2006;25:148–157.
25. Bock J, Frydrychowicz A, Stalder AF, et al. 4D phase contrast MRI at 3 T: effect of standard and blood-pool contrast agents on SNR, PC-MRA, and blood flow visualization. Magn Reson Med 2010;63:330–338.
26. Bland JM, Altman DG. Statistical methods for assessing agreement between two methods of clinical measurement. Lancet 1986;1:307–310.